Eur Radiol (2004) 14:193–200
DOI 10.1007/s00330-003-1997-2

Moshe Graif
Carlo Martinoli
Shimon Rochkind
Anat Blank
Leonor Trejo
Judith Weiss
Ada Kessler
Lorenzo E. Derchi

Sonographic evaluation of brachial plexus pathology

Received: 3 October 2002
Revised: 4 March 2003
Accepted: 2 June 2003
Published online: 5 July 2003
© Springer-Verlag 2003

M. Graif (✉) · A. Blank · J. Weiss
A. Kessler
Department of Radiology,
Tel Aviv Sourasky Medical Center
and the Sackler Faculty of Medicine,
Tel Aviv University,
6 Weizmann Street, 64239 Tel Aviv, Israel
e-mail: graif@post.tau.ac.il
Tel.: +97-2-36973504
Fax: +97-2-36974659

S. Rochkind
Department of Neurosurgery,
Tel Aviv Sourasky Medical Center
and the Sackler faculty of Medicine,
Tel Aviv University,
6 Weizmann Street, 64239 Tel Aviv, Israel

L. Trejo
Department of Pathology,
Tel Aviv Sourasky Medical Center
and the Sackler Faculty of Medicine,
Tel Aviv University,
6 Weizmann Street, 64239 Tel Aviv, Israel

C. Martinoli · L. E. Derchi
Department of Radiology,
University of Genoa,
Genoa, Italy

Abstract Pre-operative US examinations of the brachial plexus were performed with the purpose of exploring the potential of this technique in recognizing lesions in the region and defining their sonographic morphology, site, extent, and relations to adjacent anatomic structures, and comparing them to the surgical findings to obtain maximal confirmation. Twenty-eight patients with clinical, electro-conductive, and imaging findings suggestive of brachial plexus pathology were included in this study. There were four main etiology groups: post-traumatic brachial plexopathies; primary tumors (benign and malignant); secondary tumors; and post irradiation injuries. Twenty-one of the 28 patients underwent surgery. Advanced imaging (mostly MRI) served as an alternative gold standard for confirmation of the findings in the non-surgically treated group of patients. The US examinations were performed with conventional US units operating at 5- to 10-MHz frequencies. The nerves were initially localized at the level of the vertebral foramina and then were followed longitudinally and axially down to the axillary region. Abnormal US findings were detected in 20 of 28 patients. Disruption of nerve continuity and focal scar tissue masses were the principal findings in the post-traumatic cases. Focal masses within a nerve or adjacent to it and diffuse thickening of the nerve were the findings in primary and secondary tumors. Post-irradiation changes presented as nerve thickening. Color Doppler was useful in detecting internal vascularization within masses and relation of a mass to adjacent vessels. The eight sonographically negative cases consisted either of traumatic neuromas smaller than 12 mm in size and located in relatively small branches of posterior location or due to fibrotic changes of diffuse nature. Sonography succeeded in depicting a spectrum of lesions of traumatic, neoplastic, and inflammatory nature in the brachial plexus. It provided useful information regarding the lesion site, extent, and anatomic relationships; thus, the principal aims of the study were therefore met. Once the technique of examination is mastered, sonography should be recommended as part of the pre-operative evaluation process post-ganglionic brachial plexus pathology. Most disadvantages are related to the restricted field of view and inability to overcome bonny obstacles particularly in evaluating pre-ganglionic region. As sonography is frequently employed for investigation of the supraclavicular region, awareness of the radiologist to the findings described may enable the early recognition of pathologies involving or threatening to involve the brachial plexus.

Keywords Nerve · Peripheral nerve · Brachial plexus · Brachial plexopathies · Ultrasound · Nerve sheath tumors

Introduction

Magnetic resonance imaging is currently the preferred method for direct imaging of the brachial plexus [1, 2]. Computed tomographic myelography is useful in evaluating pre-ganglionic plexus pathology [3, 4].

The recent successful attempts to use US for imaging of the brachial plexus anatomy in particular [5, 6] and peripheral nerve in general [7] encouraged this prospective US study of brachial plexopathies. The aim of the current study was to explore the potential of this technique in recognizing lesions in the region of the brachial plexus, characterizing their nature and assessing their extension and relation to adjacent anatomic structures.

Materials and methods

The study population included 28 patients with clinical, electroconductive, and imaging findings suggestive of brachial plexopathy. The etiologies (see Table 1) included trauma (12 patients), primary tumors (6 patients), secondary tumors (10 patients), and post-irradiation (6 patients, 5 of them overlapping with secondary tumors and 1 patient with malignant peripheral nerve sheath tumor known as MPNST). The patients' mean age was 48 years (±18 years; age range 22–75 years).

Patterns of clinical involvement of the plexus included pain, weakness, sensory deficit, Horner's syndrome, and vasomotor changes.

The levels of the lesions as based on EMG or clinical findings were as follows: C-5 (3 lesions); C-6 (4 lesions); C-7 (5 lesions); C-8 (3 lesions); T-1 (2 lesions); lateral cord (1 lesion); medial cord (1 lesion); upper trunk (1 lesion); axillary branch (3 lesions); accessory nerve (2 lesions); suprascapular nerve (2 lesions); and ulnar nerve (1 lesion).

Table 1 Etiology of brachial plexus lesion. *MPNST* malignant peripheral nerve sheath tumor

Causes of brachial plexopathies	
Diagnosis	No. of cases
Traumatic injuries	12
Crush	5
Cervical rib (repeated compression–microtrauma)	1
Repetitive trauma (sport)	1
GSW and SW	3
Surgical biopsy (iatrogenic)	2
Primary tumors	6
Schwannoma	3
Neurofibromatosis	2
MPNST	1
Secondary tumors (metastatic)	10
Breast carcinoma	8
Mesenchymal neck tumor	1
Lung carcinoma (pancoast)	1
Radiation fibrosis	6[a]

[a] Overlapping with the group of secondary tumors (5 cases) and malignant primary tumor (1 case)

Additional imaging studies included 15 MR exams, 10 CT studies, 4 nuclear scans, and one angiographic study.

Twenty-one of the patients underwent surgery, which included exploration, decompression and removal of fibrous bands, scar tissue, traumatic neuromas, or tumors in extra-fascicular and intrafascicular locations. They underwent microsurgical external and internal neurolysis and neurotization with various grafts as well. Magnetic resonance imaging (4 patients), CT (3 patients), and positron emission tomography (PET) with fluorine-18 fluoro-2-deoxy-D-glucose (FDG) were available for confirmation of the US data in the patients that were not surgically treated.

Ultrasound examinations were performed on conventional US units equipped with color Doppler capabilities using 5- to 10-MHz linear and curvilinear transducers. The nerves were initially localized at the level of the vertebral foramina and then were followed longitudinally and transversely down to the axillary region. The identification of the normal nerve on US was based on the recognition of a hypoechoic structure tubular in shape in the longitudinal axis and round on transverse sections [5, 6, 7]. The nerves were thicker at the root level and then tapered down gradually towards the periphery. An internal linear (fascicular) pattern was just recognizable. Each root was cephalad and adjacent to the relative transverse process on longitudinal and transverse sections. The trunks located between the anterior and middle scalene muscles are best imaged on sagittal sections (Fig. 1A, B). In the retroclavicular region the nerves were located cephalad and posterior to the subclavian artery (Fig. 1C) which was easily detected and confirmed using color Doppler. Scanned along their longitudinal axes (coronal) the nerves appear as linear structures parallel to each other (Fig. 1D, E). All US examinations were performed by three radiologists (M.G., C.M., and L.E.D.). The examiners were aware of the clinical information but partially blinded to the findings of the ancillary imaging studies. Sonography was performed in the patients scheduled already for surgery (on bases of clinical, electro-physiological, and imaging findings) 24–48 h prior to surgery for the purpose of topographic correlation, skin marking of lesion location, and evaluation of surrounding vascular anatomy. Duration of the US examination stabilized at 35–40 min per side after an initial learning period (first 10–15 cases).

Results

Trauma

Three main types of ultrasound findings were detected in the trauma patients:

1. Disruption of nerve continuity (Fig. 2A) which was associated with swelling of the proximal and distal stumps and a "wavy" course of the retracted distal segment (Fig. 2B).
2. Scar tissue mass, irregular in shape and hypoechoic in texture. The mass, which is located primarily in the soft tissues, was seen to merge with one or more nerves (Fig. 3).
3. Segmental fusiform thickening of trunk of the plexus representing traumatic neuroma.

Color Doppler delineated narrowing of the subclavian artery in 1 case. No definite US findings could be detected in the other eight trauma cases. Surgical findings in these patients included three traumatic neuromas (up to

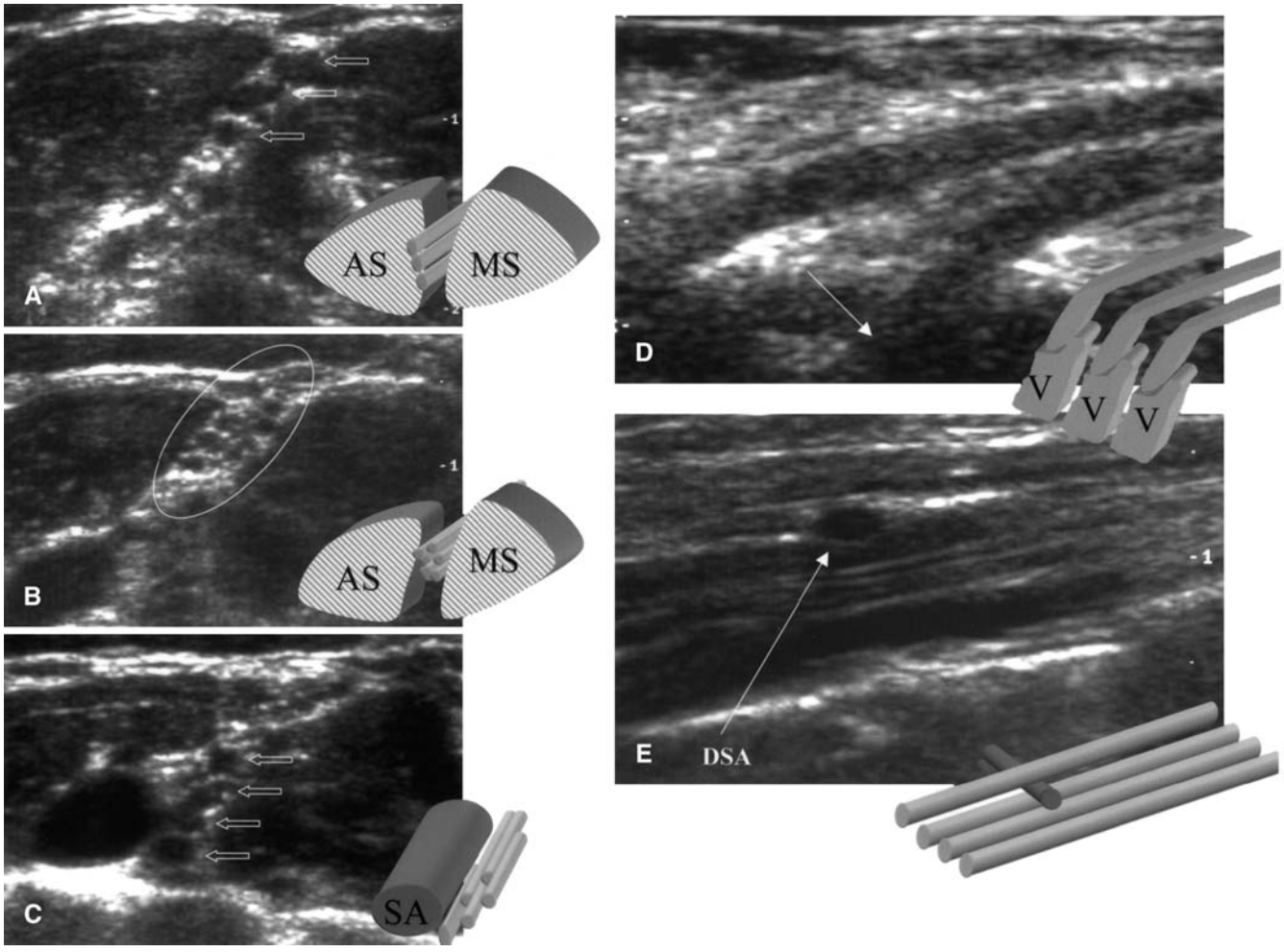

Fig. 1A–E Normal sonograms are displayed with their relative anatomic drawings. **A** Sagittal sonograms at the level of the interscalene triangle with anterior (*AS*) and middle (*MS*) scalene muscles. The trunks appear like a series of tubular structures (*arrows*). **B** Slightly lateral to **A** are the divisions of the brachial plexus (*ellipsis*). **C** More laterally the divisions (*arrows*) run in close proximity to the subclavian artery (*SA*). **D** Proximal coronal sonogram shows the roots emerging from the intervertebral foramen, displaying a bulbar appearance (*arrow*), which corresponds to the ganglia. Distally they appear as longitudinal tubular formations. **E** More laterally they run almost parallel. Note the dorsal branch of the dorsal scapular artery (*DSA*) which is perpendicular to the nerve divisions (*arrow*)

12 mm in size), four diffuse scars, and one fibrous band associated with a cervical rib in a patient with thoracic outlet syndrome.

The imaging studies available in these cases included MRI (five studies) and CT (two studies). The MRI studies depicted edema in the region of the brachial plexus in two of the studies. Signs of root avulsion at the level of the neural foramina was seen in the disruption case. Focal enhancement around the upper trunks in proximity of the foramina was observed in the patient with segmental nerve thickening after gadolinium (Gd) administration.

The other three MR cases were considered negative (as were the corresponding US studies). No direct nerve lesions were detected on CT.

Primary nerve tumors

Space-occupying lesions were detected by US in all 6 patients with primary nerve tumors. Ultrasound depicted multiple lesions in 2 patients (both neurofibromatosis type 1). The masses were globular or fusiform in shape and hypoechoic in texture (Fig. 4). The lesions in the other 3 patients with benign tumors (schwannomas) were solitary, rounded in shape with regular smooth contours (Fig. 5), and hypoechoic (2 cases) or mixed echotexture (1 case). They were in continuity with the nerve although slightly eccentric and ranged in size from 4 to 5 cm. The only primary malignant peripheral nerve sheath tumor (MPNST) presented as a diffuse hypoechic thickening of the nerve with a hypoechoic uniform pattern.

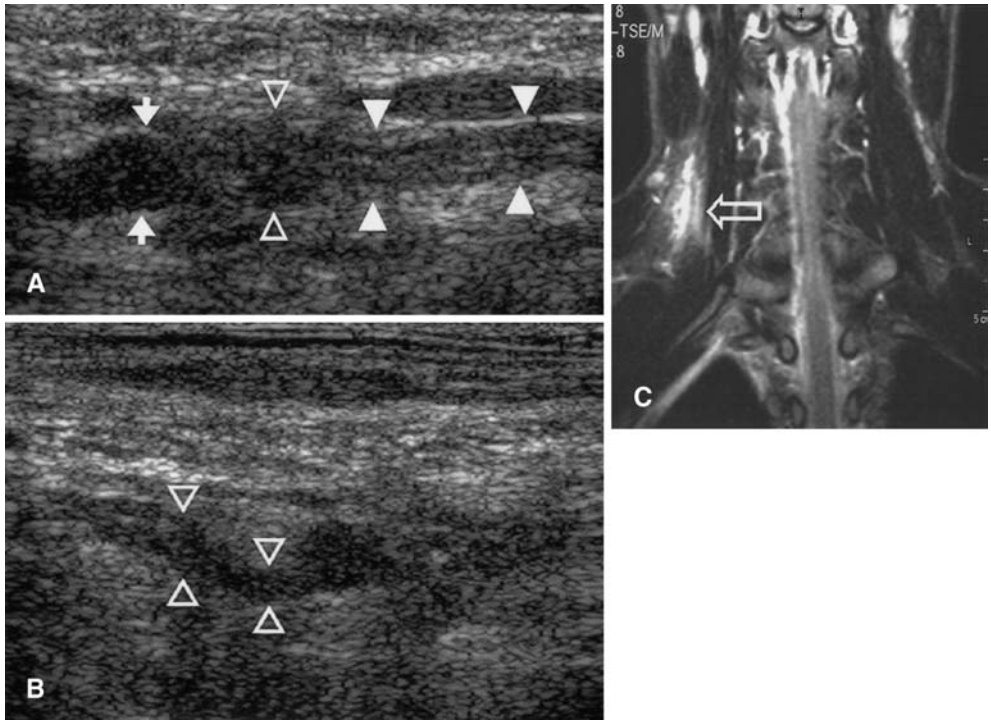

Fig. 2A–C Acute traumatic transection of the right brachial plexus in a 30-year-old man. **A** Longitudinal sonogram (5–12 MHz) obtained at the interscalene area, shows the transected nerve (C7). Note the hypoechoic swollen appearance (*open arrowheads*, *arrows*) of the proximal and distal stumps. The proximal nerve portion (*arrowheads*) appears normal. **B** A close look at the distal transected segment of the nerve shows a "wavy" appearance (*arrowheads*) due to retraction. **C** The coronal T2-weighted turbo-spin-echo MR image demonstrates an increased signal in the soft tissues of the interscalene area (*arrow*)

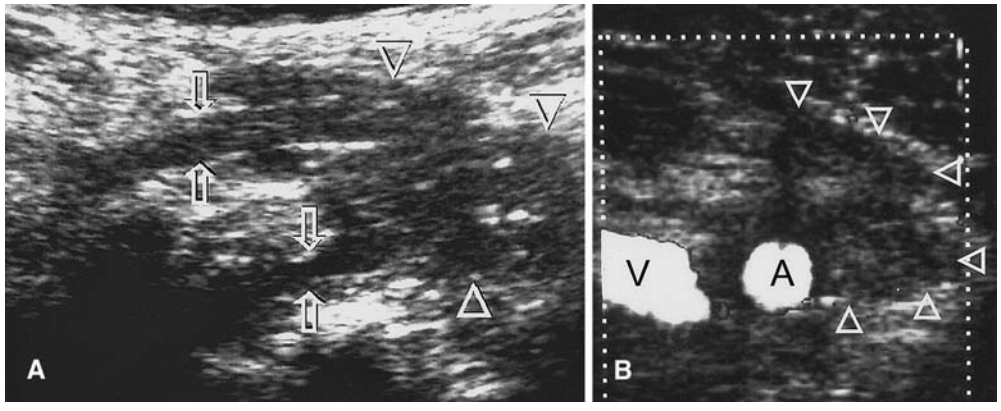

Fig. 3A, B Penetrating trauma (stab wound). **A** A left coronal (5 MHz) sonogram along the plexus demonstrates (*arrowheads*) a hypoechoic mass (scar) which involves two of the trunks (*arrows*). **B** A perpendicular (sagittal) sonogram demonstrates the scar mass (*arrowheads*), and the adjacent subclavian artery (*A*) and vein (*V*)

Internal vascularization was detected by color Doppler in all primary tumors. In one of the neurofibromatosis (NF) cases US demonstrated a rich collateral venous circulation with tortuous vessels.

Magnetic resonance imaging studies were available in all 6 patients with primary tumors and all provided information regarding the site and extent of the lesion as well as its relation to adjacent vessels. Intra-spinal involvement was shown in all three cases where present. The four CT studies yielded information similar to that provided by MRI but limited to the axial plane. In 1 case, angiography showed displacement of the subclavian artery by tumor (schwannoma). The nuclear medicine (NM) study in the same case was negative.

Secondary tumors

Hypoechoic focal mass or masses (6 of 10 patients) was the most common finding in the group of secondary tumors. Segmental fusiform thickening (Fig. 6) was the other type of finding (4 of 10 patients) observed in this group. In 3 cases both types of involvement (mass and segmental thickening) were observed concomitantly.

The nerve–tumor interface was characterized by an abrupt cutoff of the nerve course by the tumor. Enlarged lymph nodes detected in three of the patients were oval in shape, larger than 1 cm in diameter, and of medium echogenicity. Color Doppler depicted internal circulation in two of the masses. It also helped in dis-

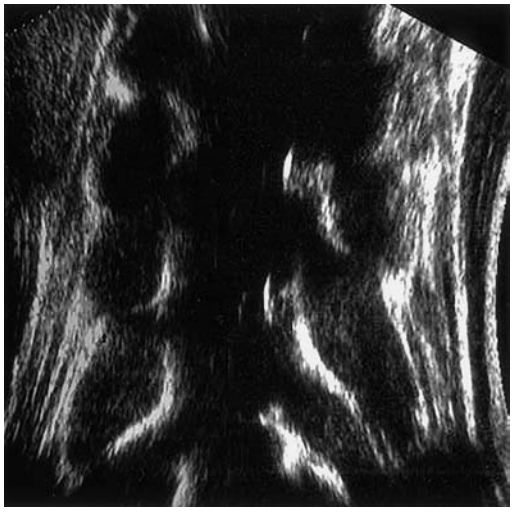

tinguishing the infiltrated cords from the adjacent blood vessels.

Ancillary imaging included MRI (4 cases) and CT (3 cases) which depicted osseous involvement (cervical vertebra) by the tumor in 1 case and pleural infiltration in another one. The MR detected the focal lesions and their relations to the brachial plexus in all cases; however, it did not demonstrate nerve thickening or textural changes in the infiltrated nerves. An FDG scan was positive in 1 case of nerve infiltration. The other NM study was negative.

Fig. 4 Neurofibromatosis type 1. Coronal sonogram (7 MHz) of the lateral neck shows a bilateral general involvement of all nerve roots and trunks by the disease. Some of the roots are globular in shape and the others fusiform (right and left coronal sonograms were fused photographically and displayed vertically)

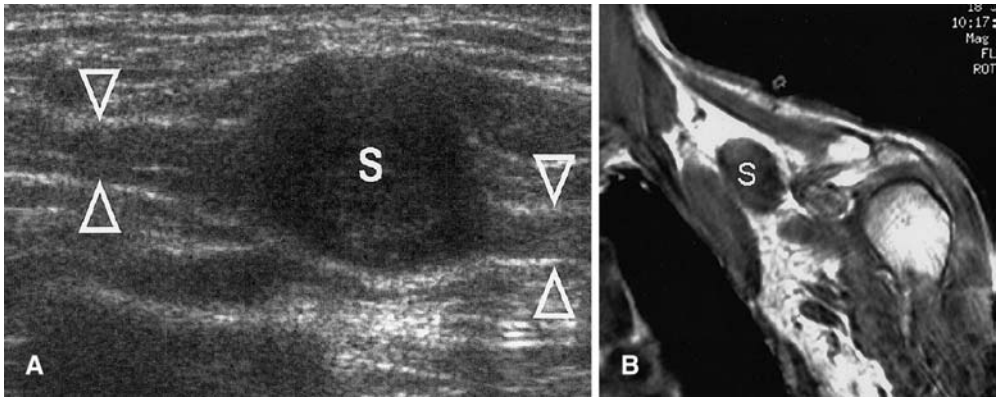

Fig. 5A, B Schwannoma of the left brachial plexus. **A** The tumor appears on ultrasound as a solitary rounded mass (*S*) with smooth contours and hypoechoic texture. *Arrowheads* mark the nerve proximal and distal to the mass. **B** Coronal T1-weighted MR image demonstrates the tumor (*S*) in the mid-portion of the supraclavicular area

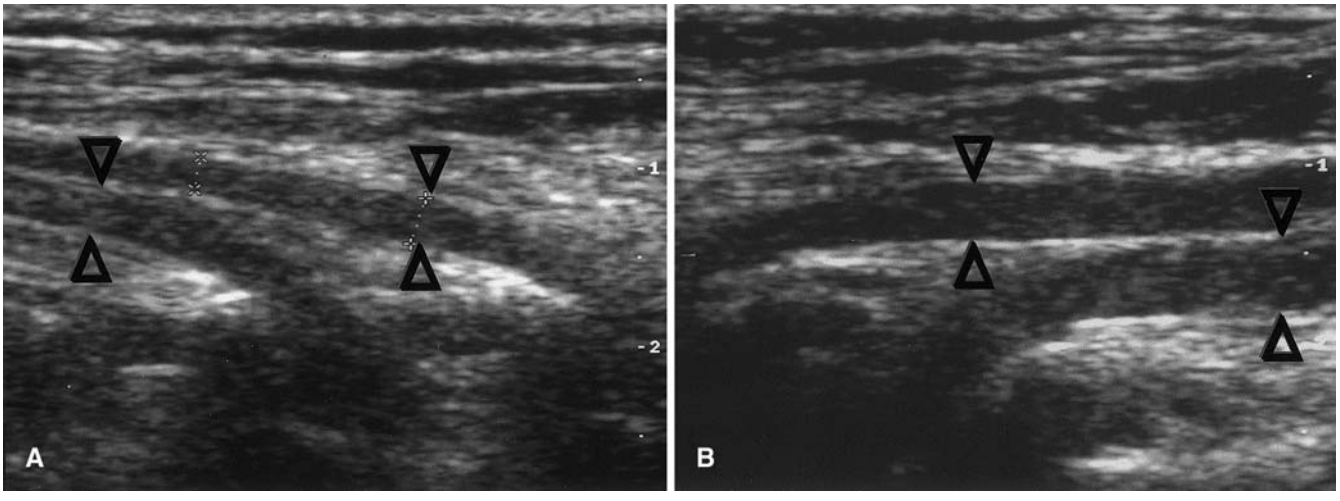

Fig. 6A, B Diffuse infiltration of nerve roots by metastatic breast carcinoma associated with post-irradiation fibrosis. **A** The right coronal sonogram shows normal appearance of C5 and C6 roots of the brachial plexus (*arrowheads*). **B** The left coronal view in the same patient shows a diffuse hypoechoic thickening of the same roots (*arrowheads*). The caliber of the affected roots is significantly enlarged in comparison with the contralateral nerves and a loss of the normal nerve tapering distally can be noted (same scaling factor on both images)

Radiation fibrosis

There was no case of isolate radiation fibrosis in this series. All cases were associated with histology of malignant disease either as a mass or cellular infiltration (5 metastatic and 1 primary malignancy). The sonographic findings included thickening and loss of tapering in one to three nerves. The caliber of the normal nerves in above-mentioned cases ranged between 0.2 and 0.4 cm. The caliber of the thickened nerve segments measured 0.5–0.95 cm, which represents a considerable increase in diameter with respect to the normal diameter. The contour showed slight irregularity and the echogenicity was reduced with loss of the internal linear texture.

Discussion

Sonography was effective in imaging normal and abnormal peripheral nerves. Two recent studies have reported successful attempts at evaluating brachial plexus anatomy using US [5, 6].

The quality of US imaging of the brachial plexus equals that obtainable by US in other peripheral nerves of similar caliber and depth. In the present study, the nerve roots could be observed on US as they exit the vertebral foramina as described in the literature (Fig. 6A). The trunks, cords, divisions, and branches of the brachial plexus could be identified and tracked down continuously to the axillary region.

In general, trauma accounts for more than half of the cases of brachial plexopathies [8]. Traumatic etiologies in this study included avulsion, penetrating wound, and iatrogenic causes (mainly surgical biopsies).

Post-traumatic nerve root disruption of the brachial plexus is usually caused by trauma mechanisms that separate the arm from the shoulder [9]. In BP stretching the most characteristic finding is pseudomeningocele which can be detected by CT and MRI [9]. Sonography is unable to visualize the internal part of the spinal canal, but, on the other hand, it has been shown to be capable of directly depicting nerve disruption and the gap between the nerve ends. Post-traumatic thickening of nerve segments probably due to neuroma was detected in 1 patient by US (and MRI) 5 months after the trauma. This information as well as distinguishing post-ganglionic from pre-ganglionic injury by EMG may be of major importance as recent advances in microsurgery permit reconstruction of nerve roots using neurotization, nerve grafting, and neurolysis [10].

All imaging modalities (US, MRI, and CT) were less successful in depicting traumatic lesions such as small traumatic neuromas (<12 mm) and diffuse fibrosis or fibrotic bands except the case of fusiform segmental thickening mentioned above. The failure to detect those lesions is probably related to a combination of factors such as the small size, insufficient contrast with the surrounding tissues, and posterior location.

Scar tissue mass secondary to penetrating trauma may appear as a focal hypoechoic mass with irregular contours. In 2 cases it was possible to delineate the location and extent of the scar mass which involved more than one cord (Fig. 3).

Neurofibromas and schwannomas are the most common neural neoplasms involving the brachial plexus. One-third of neurofibromas occur in patients with neurofibromatosis type 1 (NF-1) and two-thirds are sporadic. In NF-1 the patient tends to have multiple lesions in the brachial plexus. In the sporadic form the lesion is usually solitary. Histologically, the non-encapsulated neurofibroma is believed to arise from the nerve fascicle [11]. Sonographically, the lesion presents with well-defined contours, is homogeneous and hypoechoic, and shows internal blood vessels on Doppler. In contrast to the schwannoma, the neurofibroma has a centric course relative to the nerve. All the above-mentioned features were present in our study. Additional abnormalities depicted by US included local lymphadenopathy and the presence of a rich collateral circulation in area of the lesion, which influenced the decision regarding surgery in 1 case.

Schwannomas result from the benign transformation of Schwann cells (nerve sheath tumors). The lesions are mostly solitary and well encapsulated [12, 13]. They are located eccentrically beneath the epineurium with tendrils of the nerve splayed over the mass. The schwannomas in the brachial plexus were depicted by sonography in all our cases. The typical features, such as smooth contours, hypoechoic texture, and eccentric position (very subtle in this particular case) in relation to the nerve, were easily recognized. The echogenic capsule could not be observed due to the lack of contrast with the surrounding (mainly adipose) tissue. Internal vascularization was observed in all cases on Doppler. The MRI depicted most of the above-mentioned features as well.

Malignant peripheral nerve sheath tumor (MPNST) is a primary sarcoma arising from elements of a peripheral nerve and/or having evidence of neural differentiation [14, 15]. Our study included one case of MPNST involving the brachial plexus, The US appearance was characterized by diffuse involvement of multiple segments of the nerve (root, trunk, and division).

Tumors that have been reported to metastasize to the brachial plexus include breast, lymphoma, bladder, gastrointestinal, testicular, thyroid, lung, melanoma, head and neck, and sarcomas [16, 17]. Because one of the major lymphatic drainage routes of the breast is through the apex of the axilla, it is not uncommon for metastatic breast cancer to invade the brachial plexus. The MRI is the modality of choice for the detection of secondary invasion of the brachial plexus due to its multiplanar capabilities and high soft tissue contrast [18]. The sonographic findings reflected three patterns of involvement, focal

tumor mass, diffuse infiltration, and local lymphoadenopathy. Both MRI and CT had the advantage of a panoramic view delineating adjacent bone and pleural involvement.

Radiation fibrosis is a relatively common cause of brachial plexopathy and may account for 25% of the cases of non-traumatic plexopathies [19, 20, 21, 22]. Histologically, there is dense fibrous tissue encasing the brachial plexus with Wallerian degeneration [23]. It is somewhat difficult to discuss the sonographic aspects of radiation fibrosis, as all cases in this series were associated with malignant findings. Although features of nerve thickening were present in all the patients who underwent radiation therapy, they are far from being specific to radiation fibrosis. The sonographic demonstration of diffuse nerve thickening is similar to that described with MRI [20, 24]. Post-irradiation plexus injuries should be operated on as early as possible to stabilize the clinical course (as soon as paresthesia appears and before the onset of pain) [25]. Sonography can provide a simple, non-expensive mean to monitor caliber changes. The MRI has an advantage as it enables the distinction of radiation fibrosis from tumor infiltration on the basis of different T2 signals [19, 26, 27, 28]. The differentiation between radiation damage and residual tumor or recurrence can still be problematic as both conditions may coexist.

Conclusion

The advantages of sonography of the brachial plexus are related to its ability to directly visualize the nerve, providing fine details such as nerve disruption, detecting the presence of scar tissue, and its relation to the nerve, demarcation of changes in nerve diameter (thickening), and texture (infiltration). Visualization of tumor vascularity and adjacent circulation on US does not require the injection of contrast medium.

Sonography is easily tolerated by the patient, is cost-effective, and has been successfully applied for surgical planning either using skin markings before operation or by guiding biopsies.

The apparent disadvantages are related to the restricted field of view, which limits the panoramic topographical display. Sonography is limited in evaluating osseous or lung tissues and therefore is not able to delineate intra-spinal pathology, metastatic bone involvement, and pleural infiltration; therefore, MRI studies are needed in most cases. Acquisition of sonographic skill in assessing brachial plexus pathology requires a relatively prolonged learning curve and previous background and experience in musculoskeletal sonography.

Ultrasound provided useful information regarding the lesion site, extent, and anatomic relationships particularly to blood vessels; thus, the principal aims of the study were therefore met. Once the technique is mastered, sonography should be recommended as part of the pre-operative evaluation process post-ganglionic brachial plexus pathology. It is particularly useful in evaluation of trauma and post-traumatic changes such as irregular extensive scars. It also helps the surgeon in planning the operation and guiding diagnostic biopsies.

References

1. Hayes CE, Tsuruda JC, Mathis CM, Maravilla KR, Kliot M, Filler AG (1997) Brachial plexus: MR imaging with a dedicated phased array of surface coils. Radiology 203:286–289
2. van Es HW (2001) MRI of the brachial plexus. Eur Radiol 11:325–336
3. Montanari N, Spina V, Torricelli P, Marongiu MC, Bertolani M, de Santis M, Romagnoli R (1996) Magnetic resonance of the brachial plexus: anatomy and study technique. Radiol Med 91:714–721
4. Pierce SM, Recht A, Lingos TI et al. (1992) Long term radiation complications following conservative surgery and radiation therapy in patients with early stage breast cancer. Int J Radiat Oncol Biol Phys 23:915–923
5. Sheppard DJ, Lyer RB, Fenstermacher MJ (1998) Brachial plexus: demonstration by US. Radiology 208:402–406
6. Yang WT, Chui PT, Metreweli C (1998) Anatomy of the normal brachial plexus revealed by sonography and the role of sonographic guidance in anesthesia of the brachial plexus. AJR 171:1631–1636
7. Martinoli C, Bianchi S, Derchi LE (2000) Ultrasonography of peripheral nerves. Semin Ultrasound CT MR 21:205–213
8. Reede DL (1997) MR imaging of the brachial plexus. Magn Reson Imaging Clin N Am 5:897–906
9. Ochi L, Ikuta Y, Watanabe M, Kimori K, Itoh K (1994) The diagnostic value of MRI in traumatic brachial plexus injury. J Hand Surg (Br) 19:55–59
10. Carlstedt TP (1995) Spinal nerve root injuries in brachial plexus lesions: basic science and clinical applications of new surgical strategies. Microsurgery 16:13–16
11. England JD, Summer AJ (1996) Non traumatic brachial plexopathy. In: Wilkins RH, Rengachary SS (eds) Neurosurgery, McGraw-Hill, New York, pp 3245–3250
12. Dahl I, Hagmar B, Idvall I (1984) Benign solitary neurilemmoma (schwannoma): a correlative cytological and histological study of 28 cases. Acta Pathol Microbiol Immunol Scand 92:91
13. White W, Shin MH, Roseblum MK et al. (1990) Cellular schwannoma: a clinicopathological study of 57 patients and 58 tumors. Cancer 66:1266
14. Wanebo JE, Malik JM, Vanderberg SR et al. (1993) Malignant peripheral nerve sheath tumors: a clinicopathological study of 28 cases. Cancer 71:1247
15. Ducatman BS, Scheithauser BW, Piepgras DG (1986) Malignant peripheral nerve tumor: a clinicopathological study of 120 cases. Cancer 57:2006–2021
16. Dart LH, MacCarty CS, Love JG et al. (1970) Neoplasms of the brachial plexus. Minn Med 53:959–964
17. Lusk MD, Kline DG, Garcia CA (1987) Tumors of the brachial plexus. Neurosurgery 21:439–453

18. Castagno AA, Shuman WP (1987) MR imaging in clinically suspected brachial plexus tumor. AJR 149:1219–1222
19. Wittenberg KH, Adkins MC (2000) MR imaging of non-traumatic brachial plexopathies: frequency and spectrum of findings. Radiographics 20:1023–1032
20. Bowen BC, Verma A, Brandon AH, Fiedler JA (1996) Radiation induced brachial plexopathy: MR imaging with clinical correlation. AJNR 17:1932–1936
21. Stoll BA, Andrews JT (1966) Radiation induced peripheral neuropathy. Br Med J 1:834–837
22. Maruyama Y, Mylrea MM, Logotheis J (1967) Neuropathy following irradiation. AJR 101:216–219
23. Adams RD, Victor M (1993) Diseases of the peripheral nerves. In: Principles of neurology. McGraw-Hill, New York, pp 1117–1169
24. Posniak HV, Olson MC, Dudiak CM et al. (1993) MR imaging of the brachial plexus. AJR 161:373–379
25. Le Quang C (1993) Post-radiotherapy lesions of the brachial plexus: classifications and results of surgical treatment. Chirurgie 119:243–251
26. Glaser HS, Lee JKT, Levitt RG et al. (1985) Radiation fibrosis: differentiation from recurrent tumor by MR imaging. Work in progress. Radiology 156:721–726
27. Ebner F, Kressel HY, Mintz MC et al. (1988) Tumor recurrence vs fibrosis in the female pelvis: differentiation with MR imaging 1.5 T. Radiology 166:333–340
28. Thyarajan D, Cascino T, Harms G (1995) Magnetic resonance imaging in brachial plexopathy of cancer. Neurology 45:421–427